



Aalborg Universitet

AALBORG UNIVERSITY  
DENMARK

## Reduced junction temperature control during low-voltage ride-through for single-phase photovoltaic inverters

Yang, Yongheng; Wang, Huai; Blaabjerg, Frede

*Published in:*  
IET Power Electronics

*DOI (link to publication from Publisher):*  
[10.1049/iet-pel.2013.0734](https://doi.org/10.1049/iet-pel.2013.0734)

*Publication date:*  
2014

*Document Version*  
Early version, also known as pre-print

[Link to publication from Aalborg University](#)

*Citation for published version (APA):*

Yang, Y., Wang, H., & Blaabjerg, F. (2014). Reduced junction temperature control during low-voltage ride-through for single-phase photovoltaic inverters. *IET Power Electronics*, 7(8), 2050-2059. <https://doi.org/10.1049/iet-pel.2013.0734>

### General rights

Copyright and moral rights for the publications made accessible in the public portal are retained by the authors and/or other copyright owners and it is a condition of accessing publications that users recognise and abide by the legal requirements associated with these rights.

- Users may download and print one copy of any publication from the public portal for the purpose of private study or research.
- You may not further distribute the material or use it for any profit-making activity or commercial gain
- You may freely distribute the URL identifying the publication in the public portal -

### Take down policy

If you believe that this document breaches copyright please contact us at [vbn@aub.aau.dk](mailto:vbn@aub.aau.dk) providing details, and we will remove access to the work immediately and investigate your claim.

# Reduced Junction Temperature Control during Low-Voltage Ride-Through for Single-Phase Photovoltaic Inverters

Yongheng Yang, Huai Wang, Frede Blaabjerg

Center of Reliable Power Electronics (CORPE), Department of Energy Technology,  
Aalborg University  
Pontoppidanstraede 101, Aalborg, DK-9220 Denmark  
[yoy@et.aau.dk](mailto:yoy@et.aau.dk), [hwa@et.aau.dk](mailto:hwa@et.aau.dk), [fbl@et.aau.dk](mailto:fbl@et.aau.dk)

**Abstract**— Future photovoltaic (PV) inverters are expected to comply with more stringent grid codes and reliability requirements, especially when a high penetration degree is reached, and also to lower the cost of energy. A junction temperature control concept is proposed in this paper for the switching devices in a single-phase PV inverter in order to reduce the junction temperature stress, and thus to achieve improved reliability of a PV inverter. The thermal stresses of the switching devices are analyzed during low-voltage ride-through operation with different levels of reactive power injection, allowing an optimal design of the proposed control scheme with controlled mean junction temperature and reduced junction temperature swings. The effectiveness of the control method in terms of both thermal performance and electrical performance is validated by the simulations and experiments respectively. Both test results show that single-phase PV inverters with the proposed control approach not only can support the grid voltage recovery in low-voltage ride-through operation, but can also improve the overall reliability with a reduced junction temperature.

## I. INTRODUCTION

An imperative demand of clean and reliable electricity generation from renewable energies (e.g. photovoltaic and wind energy) has been already in effectiveness in some countries to get rid of the energy reliance on fossil-based resources [1, 2]. With the development of advanced power electronics technology, the PV systems have been a key technology to realize that demand, and will take a major part in the electricity generation soon in some areas [3]. Yet, a high penetration degree of PV systems makes the grid more decentralized and even more vulnerable. Consequently, more stringent and more specific grid requirements are going to be imposed on the future PV power systems, especially when a very high penetration level of PV power systems is coming into reality [2-9]. The future PV inverters are expected to provide a full range of functionalities like what the conventional power systems do, including ancillary services, such as frequency control through active power control, reactive power controllability and Low-Voltage Ride-Through (LVRT) capability under grid faults. For instance, the new Italian grid code requires that the generation unit with the nominal power exceeding 6 kW should have LVRT capability, and in the German E.ON grid code defined for medium- and high-voltage applications, the PV systems are required to inject reactive power during ride-through [7-11], which is shown in Fig. 1. This figure illustrates that, under a certain grid voltage level (e.g. 0.6 p.u.), a minimum reactive current (80 % of the rated grid current) should

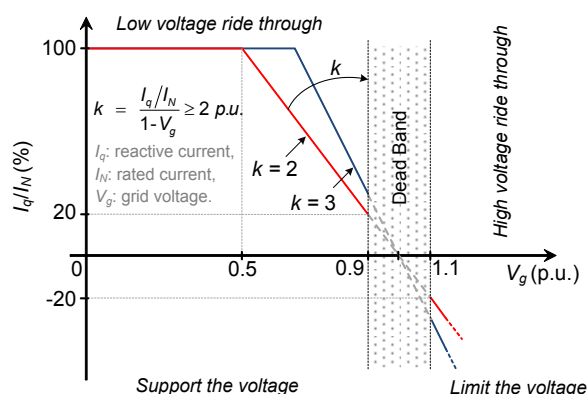


Fig. 1. Reactive current injection requirements for the power systems connected to medium- and/or high-voltage grid defined in E.ON grid code [11].

be injected into the grid to support voltage recovery. This LVRT requirement tends additionally to include all PV systems that are connected to low-voltage grids, even PV modules [4-6], since the PV systems are already on the track to dominate the electricity generation. In fact, there also have been some grid requirements for a very high penetration level of PV systems to activate reactive power control in order to solve voltage rise issues. Hence, the demand of reactive power injection will come into reality soon.

Power electronics systems (e.g. PV inverters), together with advanced control approaches, could underpin the performance of future PV systems with the provision of aforementioned ancillary services (e.g. LVRT and reactive power injection) [3-14]. The popularity of transformerless PV inverters proves that those topologies can achieve high efficiency [7, 12, 13], which is

Received on 2<sup>nd</sup> Oct. 2013. Revised on 16<sup>th</sup> Dec. 2013. Accepted on 1<sup>st</sup> Feb. 2014.

This paper is a preprint of a paper accepted by *IET Power Electronics*, and it is subject to Institution of Engineering and Technology Copyright. When the final version is published, the copy of record will be available at IET Digital Library.

DOI: 10.1049/iet-pel.2013.0734

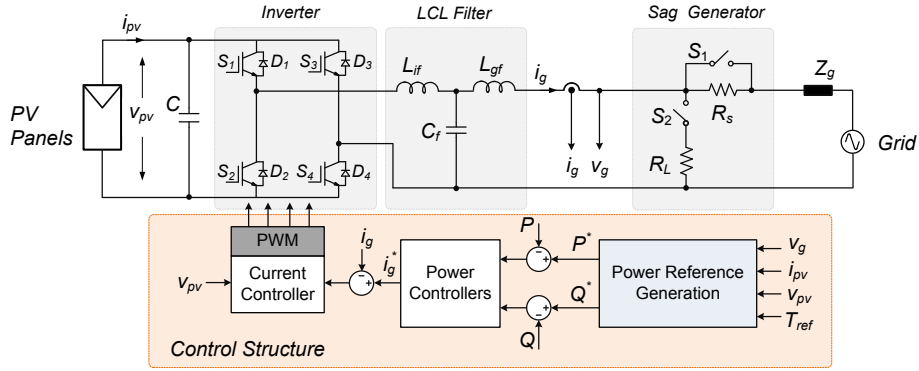


Fig. 2. Hardware schematic and control diagram of a single-phase single-stage full-bridge PV system with low voltage ride through capability to achieve a reduced junction temperature under grid faults based on single-phase PQ theory.

always of intense interest in order to reduce the cost of energy. Recently, the reliability has become another important issue for such power electronics based PV systems operating in a harsh environment, where the solar irradiance level is not constant and the grid conditions may change suddenly (e.g. voltage sag due to short-circuit faults). As it has been presented in [15], the PV inverter has been the critical part with the most failures of a PV system. Thus, it is quite necessary to predict the lifetime of a PV inverter and its components in order to improve the entire system reliability [15-22], especially when an accurate knowledge of the mission profiles (e.g. ambient temperature and solar irradiance) is available.

A PV inverter typically consists of power switching devices (e.g. IGBT and MOSFET), where various factors can contribute to the failures of them, such as thermal stress, electrical stress, mechanical stress, materials of the part and deviation in product process, and thus they affect the reliability of the entire inverter [16, 17, 23-26]. Among those factors, the most commonly observed ones are related to the thermal stresses, including the mean junction temperature and the junction temperature swings on the power switching devices [15-17]. By means of proper component selection (considering rated power, advanced packaging technologies, the most stressed situations and the severe users), effective thermal management, and robust design and validation, the reliability of a PV inverter can be improved [27-31]. Thus, in this paper, an operation mode, which can achieve a reduced junction temperature, is addressed for single-phase PV inverter during ride-through operation. This control method is based on an appropriate thermal management by properly allocating the reactive power and the active power in LVRT operation mode.

This paper is organized as follows: the viability of the proposed junction temperature control method is illustrated in § II, including the LVRT requirements and possible reactive power injection strategies. It is followed by some implementation examples. In § III, the analysis is firstly demonstrated on a 3 kW single-phase full-bridge inverter in a given operation condition (irradiance level: 1000 W/m<sup>2</sup>, ambient temperature: 50 °C) by simulations. Then, the LVRT operation mode is tested experimentally in a 1 kW grid-connected system, which can indirectly reflect that the junction temperature is dependent of the injected reactive power and the generated active power. Furthermore, a thermal experimental test is conducted on a single-phase 3-level Neutral Point Clamped (NPC) PV inverter to directly show the junction temperature controllability through power regulations. All the test results have shown that the

proposed method offers the possibility to achieve a reduced or even a constant junction temperature, which is independent of the operation conditions. The adoption of the proposed control method can help the next generation advanced PV inverters to fulfill the upcoming grid demands in terms of efficiency, stability and reliability.

## II. REDUCED JUNCTION TEMPERATURE CONTROL

### A. System Description and Requirements

Since the PV systems are still dominantly for residential applications at present, single-phase topologies are more widely used solutions for PV systems [7, 12]. Fig. 2 represents the hardware schematic of an LCL-filter based single-phase single-stage full-bridge PV system with the proposed control structure. Standard functionalities for a PV inverter are a) optimization/maximization of the input power, b) manipulation of the inverter output voltage (i.e. voltage control), and c) synchronization with the grid voltage [3, 7, 12]. Hence, in normal operation, the system is required to inject the maximum active power, known as Maximum Power Point Tracking (MPPT) control and typically, the MPPT control can be enhanced by integrating a boost stage between the PV panels and the inverter shown in Fig. 2. Moreover, the injected grid current should have less harmonic components, which is referred as Total Harmonic Distortion (THD). In normal operation mode, the PV system is required to operate at a minimum Power Factor (PF) of 0.85, and the injected current THD should be lower than 5 % [7, 8]. Traditionally, in response to a grid variation, e.g. a voltage sag or a frequency disturbance, the PV systems should disconnect from the grid in order to prevent from islanding operation [4]. However, with an even higher installation rate of PV systems, the disconnection of a considerable amount of PV systems unintentionally will further induce frequency instability (grid variations), leading to more serious events, e.g. power outage and voltage flickering.

To solve this issue, the grid codes have been updated to enable LVRT capability for PV systems. Moreover, recent studies have shown the beneficial contributions of LVRT for PV systems to distributed grid stability, conversion efficiency and reliability [2-3, 6-9]. To perform LVRT functionality, the PV system should have the controllability to remain connected and also to support the grid voltage with reactive power injection when a voltage fault is confirmed. In other words, the PV system should switch the mode of operation from MPPT to LVRT by monitoring the grid voltage amplitude. However, with the reallocation of the injected reactive power and active power

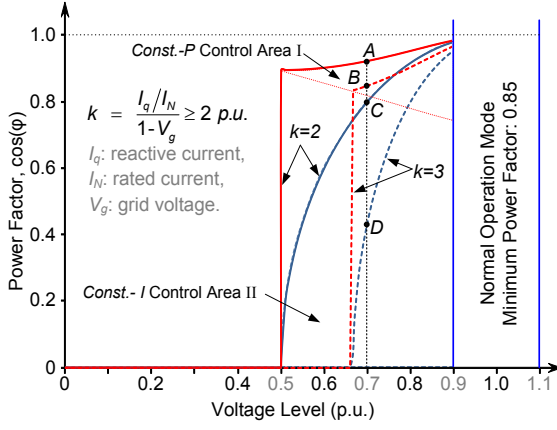


Fig. 3. Power factor curves vs. voltage levels for different control strategies according to Fig. 1: solid lines:  $k = 2.0$  and dashed lines:  $k = 3.0$ .

during LVRT, the current stresses as well as the power losses are changed, leading to a redistribution of the thermal stresses on the power switching devices. Thus, the junction temperature of the power devices can be manipulated indirectly, which offers a possibility to achieve a reduced or constant junction temperature, and thus also an improved lifetime, which has been an important requirement for power electronics based PV systems.

The viability of this principle is demonstrated by (1) and (2), where an example of the IGBT lifetime model is presented [31].

$$N_f = k \cdot (\Delta T_j)^{\beta_1} \cdot e^{\frac{\beta_2}{T_{j\_mean}}} \cdot (t_{ON})^{\beta_3} \cdot i^{\beta_4}, \quad (1)$$

$$T_j = f(i, v, T_a, f_s, p_{loss}, \dots), \quad (2)$$

with  $N_f$  being the cycle-to-failure numbers,  $k, \beta_{1,2,3,4}$  being the coefficients related to the device material,  $t_{ON}$  is the switching pulse width, and  $i$  being the wire current. As it has been shown in (1), the lifetime of a power device is significantly affected by the junction temperatures, including the cyclic temperature  $\Delta T_j$  and the mean temperature  $T_{j\_mean}$ . Moreover, it is observed in (2) that the junction temperature  $T_j$  is a function of various factors, e.g. current level,  $i$ , voltage stress,  $v$ , and ambient temperature,  $T_a$ , switching frequency  $f_s$ , and the power losses,  $p_{loss}$ . Since the power losses are dependent on the inverter topology and thus the ratio between the generated active power and the injected reactive power, an appropriate allocation of reactive power can possibly contribute to the reliability improvement.

### B. Reactive Power Injection Strategies

Regarding the reactive power injection strategies for single-phase systems, there are three reactive power control strategies proposed in [7] – constant peak current strategy, constant active power strategy, and constant active current control strategy. Those strategies can inject sufficient reactive power, which is dependent on the voltage sag level, but with different control objectives. Here, two strategies (constant peak current control and constant active power control) are selected in order to illustrate the principle of the proposed method. Both strategies are in compliance with the grid codes shown in Fig. 1.

#### Constant Peak Current Strategy – Const.-I

The injected grid current is kept to be the nominal (rated) current ( $I_N$ ) during ride-through operation for this control strategy. Then, according to Fig. 1, the active current ( $I_d$ ) and reactive current ( $I_q$ ) in the  $dq$ -rotating reference frame are calculated as,

$$\begin{cases} I_d = I_N \sqrt{1 - k^2 (1 - V_g)^2} \\ I_q = k (1 - V_g) I_N \end{cases} \quad (3)$$

in which  $V_g$  is the grid voltage level in p.u.,  $k$  is the slope defined previously in Fig. 1 and it has a minimum value of 2 p.u., and  $(1 - 1/k)$  p.u.  $\leq V_g < 0.9$  p.u.. When a deep voltage sag occurs ( $V_g < (1 - 1/k)$  p.u.), according to Fig. 1, the PV system should inject full reactive power to the grid. For example, when  $k = 2$  p.u. and the grid voltage goes below 0.5 p.u., the current should be  $I_d = 0$  A and  $I_q = I_N$ . Based on (3), the corresponding power factor in LVRT operation mode can be expressed as,

$$\begin{aligned} \cos \varphi &= \frac{P}{S} = \frac{P}{\sqrt{P^2 + Q^2}} \\ &= \begin{cases} \sqrt{1 - k^2 \cdot (1 - V_g)^2}, & \left(1 - \frac{1}{k}\right) \text{ p.u.} \leq V_g < 0.9 \text{ p.u.} \\ 0, & V_g < \left(1 - \frac{1}{k}\right) \text{ p.u.} \end{cases} \end{aligned} \quad (4)$$

where  $S$  is the instantaneous apparent power.

#### Constant Active Power Strategy – Const-P

In this control strategy, the injected reactive current is calculated based on Fig. 1 and the active power is kept to be the nominal value ( $P_n$ ). The major purpose of this control strategy is to deliver as much energy as possible to the grid, even in the case of a grid voltage sag. Hence, according to the single-phase  $PQ$  theory, the current in  $dq$ -rotating reference frame is given as,

$$\begin{cases} I_d = \frac{1}{V_g} I_N \\ I_q = k (1 - V_g) I_N \end{cases} \quad (5)$$

However, with *Const.-P* control strategy, the current level may exceed the limitation of the PV inverter ( $I_{max} \leq \sqrt{I_d^2 + I_q^2}$ ), leading to inverter shutdown due to over-current protection. To prevent the inverter from over-current shutdown, the following condition should be satisfied,

$$\frac{1}{V_g} \sqrt{1 + k^2 \cdot (V_g - V_g^2)^2} \leq \frac{I_{max}}{I_N}, \quad (6)$$

where  $(1 - 1/k)$  p.u.  $\leq V_g < 0.9$  p.u., and  $I_{max}$  is the inverter allowable current level. Similar to constant peak current control strategy, when a deep voltage sag happens, the system should inject full reactive power to the grid, and meanwhile the active power generation should be deactivated.

For this control strategy, the PF can be expressed as,

$$\begin{aligned} \cos \varphi &= \frac{P_n}{S} = \frac{P_n}{\sqrt{P_n^2 + Q^2}} \\ &= \begin{cases} 1 / \sqrt{1 + k^2 \cdot (V_g - V_g^2)^2}, & \left(1 - \frac{1}{k}\right) \text{ p.u.} \leq V_g < 0.9 \text{ p.u.} \\ 0, & V_g < \left(1 - \frac{1}{k}\right) \text{ p.u.} \end{cases} \end{aligned} \quad (7)$$

where  $k$  is defined previously,  $P_n$  is the nominal active power and  $S$  is the apparent power.

Although the *Const. - P* control can output the maximum power in different operation modes, it is known from (6) that the *Const. - P* control strategy can only be adopted when  $I_{\max} \geq 2.236 I_N$  with  $k$  being 2.0 p.u., which is very large for the inverter design and will increase the cost of the PV inverter. Moreover, an inappropriate design margin (e.g.  $I_{\max} = 1.5 I_N$ ) may cause the power devices more easily to fail when a grid fault happens. Whilst for the *Const. - I* control, the peak value of the injected grid current is kept constant during operation, and thus there is no risk of over-current shutdown.

### C. Reduced Junction Temperature Control

Based on the previous discussions, the thermal performance of a PV inverter is affected by the power losses, which are dependent on the grid conditions and the power allocations. Under different control strategies, the ratio between the active power and the required reactive power is varied, and thus the power factor. Therefore, the junction temperature is affected. According to (4) and (7), the control areas for these two strategies under grid faults can be plotted in Fig. 3. The upper borders (solid lines) of the control areas (I and II) are the maximum power factor ( $k = 2$ ) that is required under grid faults according to Fig. 1. Thus, in these control areas (I and II), the active power and reactive power can be allocated properly and intentionally, and varied by adjusting the slope  $k$  or by changing the control strategies. As aforementioned, this will lead to a redistribution of the power losses on the switching devices, and thus offers the control possibility to achieve a reduced or constant junction temperature by optimizing the active power and reactive power in those areas. This is the main idea of the proposed control method in order to achieve a constant or reduced junction temperature of the power devices.

For example, as it is shown in Fig. 3, a voltage sag (0.3 p.u.) occurs and the *Const. - I* control strategy is firstly activated once the voltage sag is detected. In this case, the required power factor should be approximately 0.8 when  $k = 2$  p.u.. By adjusting  $k$  to 3 p.u. or changing the mode of control to *Const. - P* control strategy, the operation points will change from  $C$  to  $D$  or from  $C$  to  $A$ , and thus the injected active power and reactive power are manipulated, leading to a change of loss distribution on the power devices. According to (2) and previous discussions, since the power losses have a significant impact on the thermal behavior of the power devices, a manipulation of the junction temperature is achieved by varying  $k$  or changing the control strategies.

The control philosophy of the proposed method has been illustrated in the last paragraph. A detailed implementation of this control strategy is shown in Fig. 4. By optimizing the power references ( $P^*$  and  $Q^*$ ) shown in Fig. 2 according to voltage sag depths, an allocation of the powers can be done and thus the control goals can be achieved. As it is shown in Fig. 4, the proposed control method can not only meet the reactive power injection requirement but also enhance the reliability performance by means of controlling the power device junction temperature through active and reactive powers exchanging with the grid. The key of the implementation of this control method is to find the optimum power references under different grid levels by means of look-up tables or mathematical derivations. Thus, an appropriate thermal model of the power devices is necessary, since the electrical model of the power devices is coupled with the thermal model through the power losses on the device [24, 25].

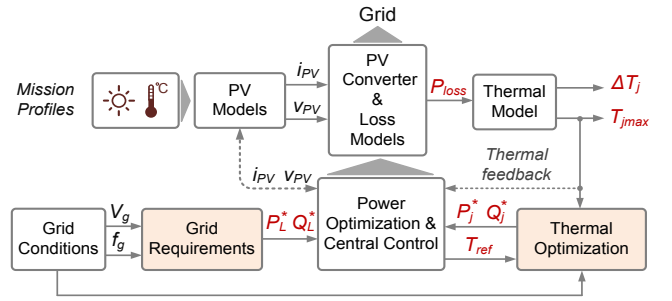


Fig. 4. Control structure of the proposed junction temperature control method through active power and reactive power regulation.

Fig. 5 shows a thermal model of the power devices, where  $Z_{th}$  is the thermal impedance between two nodes. It is illustrated in Fig. 5 that the power losses ( $P_{tot(S)}$  and  $P_{tot(D)}$ ) on the power devices will cause temperature rise at different nodes because of the thermal impedances. This relationship can be described as,

$$\begin{aligned} T_{j(S/D)}(t) &= P_{tot(S/D)}(t) Z_{th(S/D)(j-c)}(t) + T_c(t) \\ &= P_{tot(S/D)}(t) Z_{th(S/D)(j-c)}(t) \\ &\quad + [P_{totS}(t) + P_{totD}(t)] \cdot [Z_{th(c-h)}(t) + Z_{th(h-a)}(t)] \\ &\quad + T_a(t) \end{aligned} \quad (8)$$

in which,  $T_{j(S/D)}$  is the IGBT/diode junction temperature,  $P_{tot(S/D)}$  is the IGBT/diode total losses,  $Z_{th(S/D)(j-c)}$  is the thermal impedance from junction to case,  $Z_{th(c-h)}$  is the thermal impedance from case to heat-sink,  $Z_{th(h-a)}$  is the thermal impedance from heat-sink to ambient,  $T_c$  is the case temperature, and  $S$  represents the IGBT and  $D$  denotes the diode. Typically, the thermal impedance can be modeled as a multi-layer Foster model [28, 33-35], which is a series-connected model as shown in Fig. 5, and it can be expressed as,

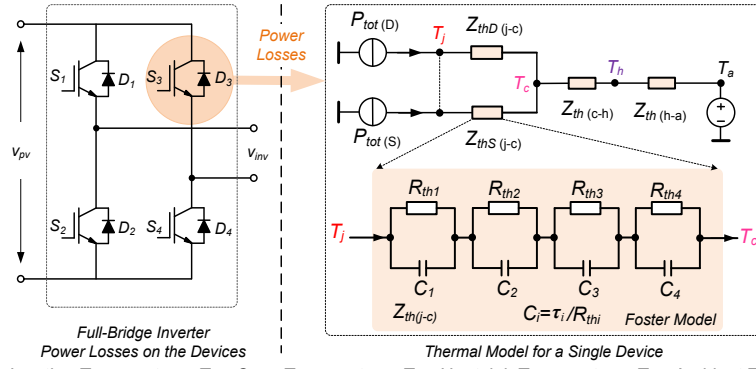
$$Z_{th(S/D)}(t) = \sum_{i=1}^4 R_{thi} (1 - e^{-t/\tau_i}), \quad (9)$$

with  $\tau_i = C_i R_{thi}$ . Those parameters in (9) can be found in the datasheet. It is shown in (8) and (9) that the junction temperature is dependent on the dissipated power. This also implies the viability of the proposed method.

### D. Implementation for the Proposed Method (Power References)

Regarding the implementation of the proposed method, there are two possibilities to obtain the power references, which are dependent on the voltage sag level. One method is based on mathematical derivations, and it requires a better knowledge of the power device materials, the topologies, the switch schemes, and etc.. Meanwhile, the coupled relationship between power losses and the junction temperature further increase the derivation complexity. An alternative is based on look-up tables, although at a cost of the accuracy. This method is simple and can easily be implemented. Thus, in this paper, the look-up table based implementation method is chosen for a single-phase PV system.

To create a satisfied look-up table and thus to find the optimum power references for the proposed method, different cases (varying allocations of reactive power and active power) should be studied first. Referring to Fig. 2, a 3 kW single-phase system is simulated under various active power levels with reac-



Notes:  $T_j$  – Junction Temperature,  $T_c$  – Case Temperature,  $T_h$  – Heatsink Temperature,  $T_a$  – Ambient Temperature;

Fig. 5. Thermal models from a full-bridge PV inverter in Fig. 2 to a single power device and the thermal impedance [26, 32-34].

-tive power injection when a low-voltage fault occurs. The results are presented in Fig. 6, where it is noted that the maximum junction temperature ( $T_{jmax}$ ) of the power devices will exceed the allowable value (e.g. 125 °C) under very low voltage conditions (e.g. 0.4 p.u.). It also reveals that the maximum junction temperature will increase with injecting required reactive power in *Const. -P* control mode. By decreasing the active power output and limiting the reactive power injection, the maximum junction temperature could be controlled below a desirable value (e.g.  $T_{jmax,d} = 80$  °C) and thus can be kept almost constant during ride-through. Considering the required reactive power injection in Fig. 1, the active power and reactive power references can be obtained as shown in Fig. 7 (a) under different voltage sag levels. While for a constant junction temperature of 80 °C, based on Fig. 6, the power references can be obtained and shown in Fig. 7 (b). Consequently, the reference generation zones can be implemented as the “Power Reference Generation” unit in Fig. 2. In the detailed control structure of the proposed method in Fig. 4, the power references for LVRT requirements (Fig. 7 (a)) and constant junction temperature (Fig. 7 (b)) can be implemented as the “Grid Requirements” and “Thermal Optimization” units respectively.

For instance, when the grid sags to be 0.6 p.u., there are several sets of power references available in Fig. 7 (b) - 1)  $P^*_j = 0.2$  p.u.,  $Q^*_j = 0.68$  p.u., 2)  $P^*_j = 0$  p.u.,  $Q^*_j = 0.68$  p.u., and 3)  $P^*_j = 0$  p.u.,  $Q^*_j = 1.0$  p.u.. For the first case, the active power should

be 0.2 p.u. (Point B in Fig. 7 (a)). One way to generate this active power is to change the slope  $k$ , being 2.36 p.u., while the corresponding reactive power  $Q^*_L = 0.57$  p.u. (Point D in Fig. 7(a)). This reactive power is insufficient to keep the junction temperature constant as shown in Fig. 7(b) (Point A), and thus, the maximum junction will be lower than  $T_{jmax,d}$ . If the required reactive power ( $Q^*_j = Q^*_L = 0.68$  p.u.) is injected to the grid, the peak value of the injected current will not be constant during LVRT, but the maximum junction temperature will be kept constant. Another way to achieve a constant junction temperature is to further decrease the active power generation either by increasing  $k$  or changing the reactive power injection strategies (from A to C), as it is shown in Fig. 7.

According to Fig. 6, the junction temperature of the power devices of a full-bridge inverter is proportional to the injected reactive power and the generated active power. Thus, to ensure a reduced junction temperature and considering the grid requirements, the power references optimized by the central control unit in Fig. 4 can be given as,

$$\begin{cases} P^* = \min\{P_L^*, P_J^*\} \\ Q^* = \min\{Q_L^*, Q_J^*\} \end{cases} \quad (10)$$

Consequently, the control flowchart of the proposed method is shown in Fig. 7 (c). It should be pointed out that, by applying curve-fitting to Fig. 7 (b), the power references can be formulized.

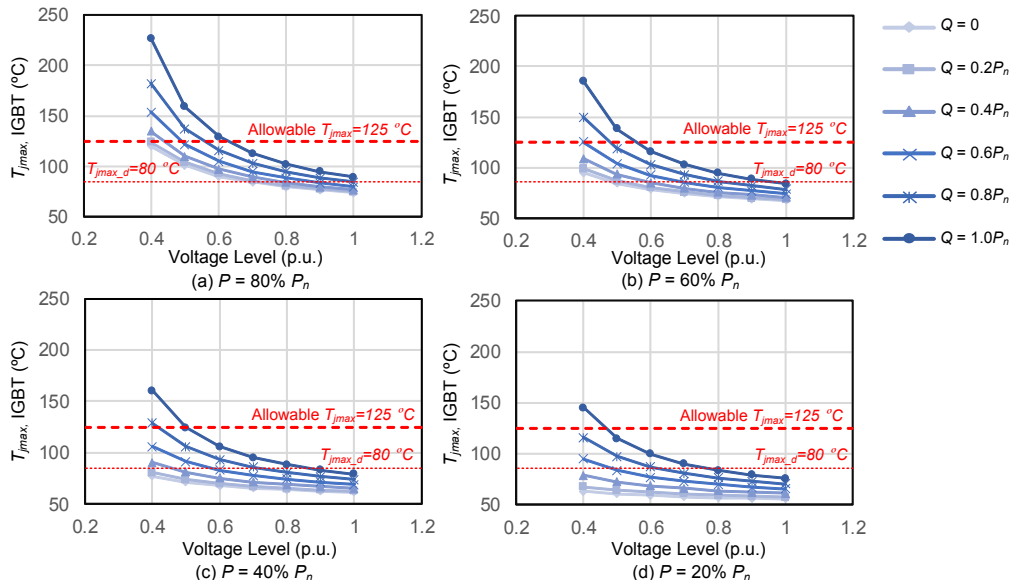


Fig. 6. Maximum junction temperature ( $T_{jmax}$ ) of a full-bridge inverter ( $P_n = 3$  kW) under grid faults with different reactive power injection.

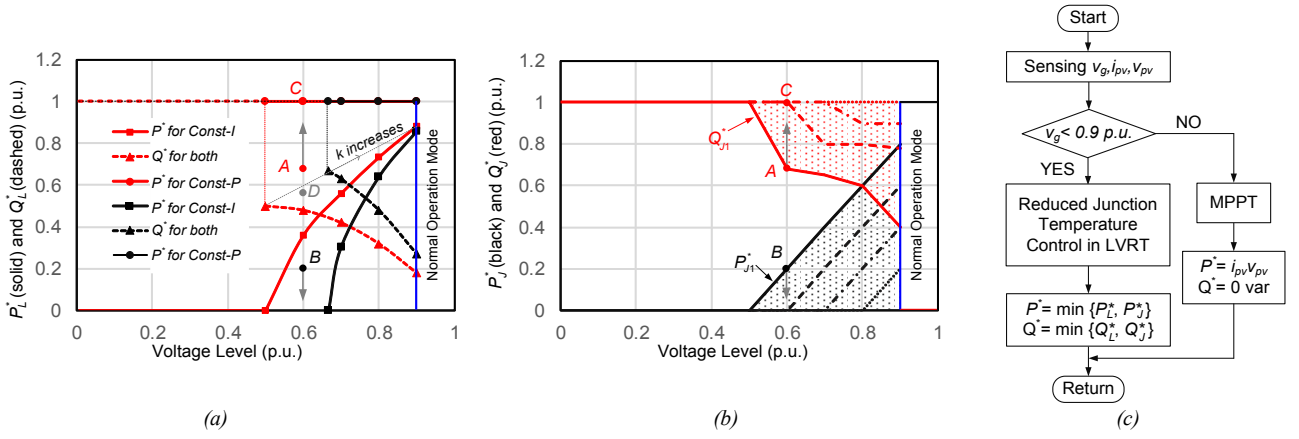


Fig. 7. Reactive power and active power references for a PV inverter: (a) to comply with the grid requirement of reactive power injection during LVRT, “L” - LVRT,  $k=2$  p.u. (red) and  $k=3$  p.u. (black) in respect to Fig. 1, (b) to achieve a constant junction temperature ( $T_{max,d} = 80$  °C), “J” - Junction and (c) flowchart of the proposed junction temperature control method.

### III. SIMULATION AND EXPERIMENTAL RESULTS

#### A. Simulation Tests

As it is discussed above, by adjusting the active power and reactive power according to Fig. 7 and (10), a reduced or even constant junction temperature operation can be achieved for single-phase grid-connected PV inverter. The hardware and overall control structure of the single-phase PV system is shown in Fig. 2. Instead of PV panels, a DC source is used in this system on the assumption that the MPPT control is very robust. The proposed control method shown in Fig. 7 was implemented in MATLAB/Simulink. A 0.43 p.u. voltage sag is generated in the simulations. The second-order generalized integrator based phase locked loop [7] is adopted to synchronize the current with the grid voltage. In order to directly and intuitively control the active power and reactive power, the single-phase  $PQ$  control method is adopted in this system. A proportional resonant current controller with harmonic compensators has been selected in order to guarantee a good power quality. An IGBT module (600 V, 50 A) from a leading manufacturer is selected with the thermal parameters shown in Table I. The other specifications of the system are listed in Table II.

Table I.  
FOSTER THERMAL PARAMETERS FOR AN IGBT MODULE FROM A LEADING MANUFACTURER.

Impedance		$Z_{th(i-c)}$				$Z_{th(c-h)}$
		1	2	3	4	
IGBT	$R_{thi}$ (K/W)	0.074	0.173	0.526	0.527	0.7
	$\tau_i$ (s)	0.0005	0.005	0.05	0.2	0
Diode	$R_{thi}$ (K/W)	0.123	0.264	0.594	0.468	0.7
	$\tau_i$ (s)	0.0005	0.005	0.05	0.2	0

Table II.  
SIMULATION PARAMETERS FOR A SINGLE-PHASE GRID-CONNECTED PV SYSTEM.

Nominal Grid Voltage	$V_{g,RMS} = 230$ V
Nominal Grid Frequency	$f = 50$ Hz
Rated Power	$P_n = 3$ kW
Nominal DC Voltage (PV Output Voltage)	$V_{dc} = 400$ V
Switching Frequency	$f_{sw} = 10$ kHz
LCL Filter	$L_{lf} = 3.6$ mH, $C_f = 2.35$ $\mu$ F, $L_{lg} = 4$ mH
Grid Impedance	$L_g = 50$ $\mu$ H, $R_g = 0.1$ $\Omega$

The power losses and the cyclic temperature on the power devices of a 3 kW single-phase PV system are firstly tested for constant junction temperature control. When a voltage fault (0.43 p.u.) is detected, the system can immediately be changed to the proposed control operation mode from normal operation condition with the MPPT control. For comparison, the LVRT operation mode with  $Const. - P$  and  $Const. - I$  control strategies are also simulated. The results are shown in Table III and Fig. 8.

As it can be observed in Fig. 8(a), although the LVRT operation with  $Const. - P$  control strategy can also inject the required reactive power, the injected grid current level is about 2.0 p.u. during LVRT. The high current amplitude will lead to a higher power losses and thus according to (2) the mean/maximum junction temperature will increase significantly in LVRT operation, which has been verified by the results presented in Table III and Fig. 8(a). By applying the proposed junction temperature control, the power losses on the switching devices of a single-phase PV system are significantly reduced in LVRT operation mode, as it is shown in Table III. The resultant

Table III.  
POWER LOSS DISTRIBUTIONS OF THE IGBT MODULES OF A 3 kW SINGLE-PHASE PV INVERTERS IN DIFFERENT OPERATION MODES (UNIT: W).

Module No.	1		2		3		4	
	$S_1$	$D_1$	$S_2$	$D_2$	$S_3$	$D_3$	$S_4$	$D_4$
Normal Operation (MPPT)	19.2	3.1	18.95	3.1	18.95	3.1	19.2	3.1
Low Voltage Ride-Through ( $Const. - P$ , 0.43 p.u.)	48.1	13.6	47.65	13.47	47.65	13.47	48.1	13.6
Constant Junction Temperature Control (0.43 p.u.)	18.7	8.1	18.4	8.0	18.4	8.0	18.7	8.1

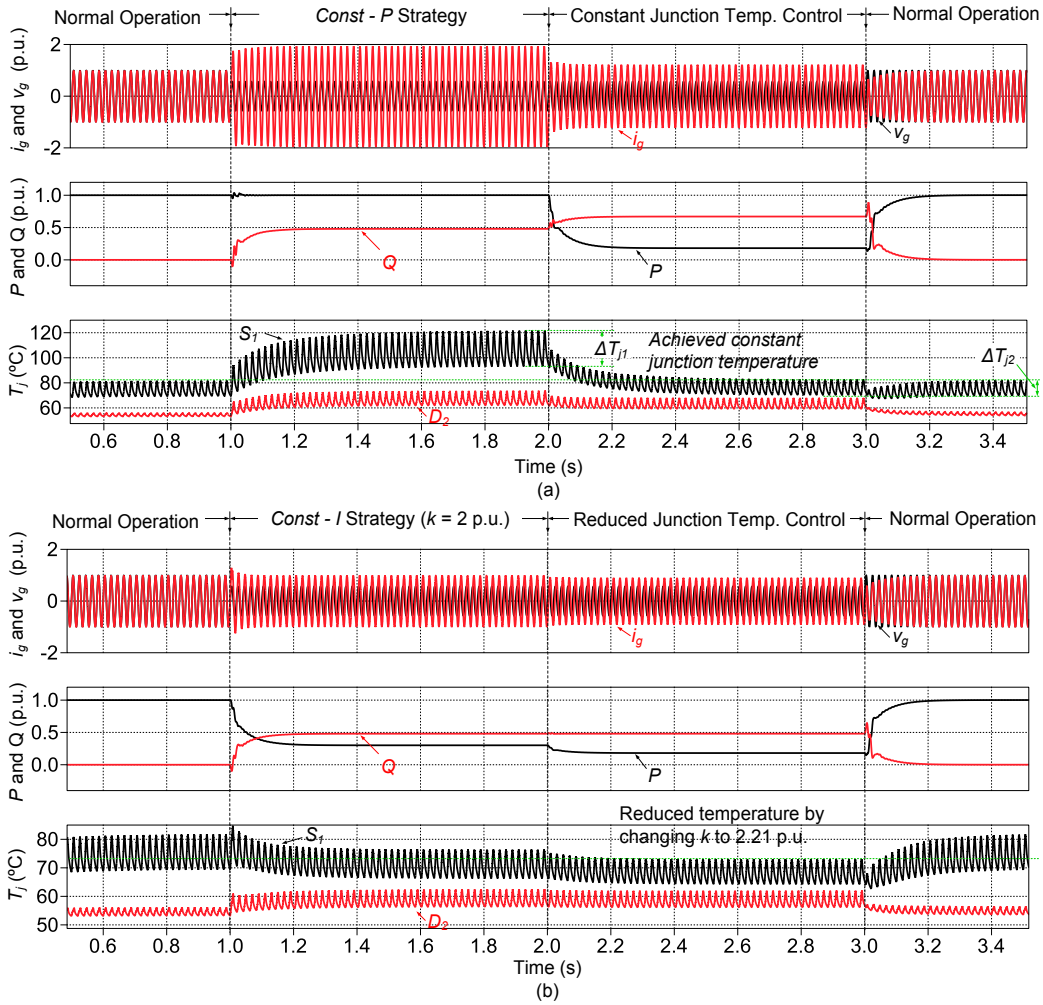


Fig. 8. Simulation results of a 3 kW single-phase full-bridge PV inverter with the proposed control method to: (a) achieve constant maximum junction temperature and (b) reduce junction temperature (voltage sag depth: 0.43 p.u.):  $i_g$ : grid current,  $v_g$ : grid voltage,  $P$ : injected active power to the grid,  $Q$ : injected reactive power to the grid,  $T_j$ : junction temperature,  $S$ : IGBT,  $D$ : diode.

lower power losses lead to a reduced mean/maximum junction temperature compared to the case in *Const. - P* mode during ride-through, as it is proved in Fig. 8(a). Moreover, the IGBT temperature cycling amplitude is also reduced to 10 °C ( $\Delta T_{j2}$ ) from 30 °C ( $\Delta T_{j1}$ ), when the system is controlled in *Const. - P* mode as it is shown in Fig. 8(a). Thus, with the proposed control method, a constant maximum junction temperature is achieved during ride-through with sufficient reactive power injection, and thus the overall reliability of the PV system is further improved according to (1). However, it can be noted from Fig. 8(a) that during ride-through the diode junction temperature is increased due to the injection of reactive power into the grid. The diode junction temperature might also be reduced or by applying the constant junction temperature control. In that case, the control objectives of the entire system during LVRT will be: 1) to ride-through low voltage condition, 2) to keep the IGBT junction temperature constant and 3) to reduce the thermal stress on the diode. Similar power reference profiles (Fig. 7) can be obtained in order to achieve these goals.

Fig. 8(b) shows the results of a 3 kW system with the proposed control method to achieve a reduced junction temperature during LVRT. By adjusting the slope  $k$ , the maximum junction temperature is reduced during LVRT. Compared with the constant junction temperature control and the *Const - I* control strategy, the proposed control method can fulfill the requirement of power injection requirement and also improve

the reliability of the entire system, since the power references for this control method are optimized according to Fig. 7 and (10). Those results show the effectiveness of the proposed method to achieve a reduced or even a constant junction temperature of the power devices under grid faults.

### B. Experimental Verifications

In order to demonstrate the ability of reactive power injection under grid faults for future PV inverters, a 1 kW grid-connected system is examined in the laboratory based on single-phase  $PQ$  theory [7, 30]. The sag generator is used to make a 0.43 p.u. voltage sag in the experiments. The proportional resonant controller with harmonic compensators is adopted again to achieve high power quality of the injected current. Except for the grid impedance, the other parameters of the experimental setup are the same as the specifications of the simulation system listed in Table II. The experimental results are presented in Fig. 9. During the LVRT operation shown in Fig. 9, the single-phase system is injecting reactive power into the grid according to grid requirements defined in Fig. 1. At the same time, the active power is reduced in order to achieve a reduced junction temperature of the IGBT devices. When the voltage fault is cleared (the voltage amplitude goes to 90% of the nominal value), the system returns to its normal operation mode and it is injecting satisfactory current at unity power factor. Since the *Const - I* control strategy is adopted in the experiments, this



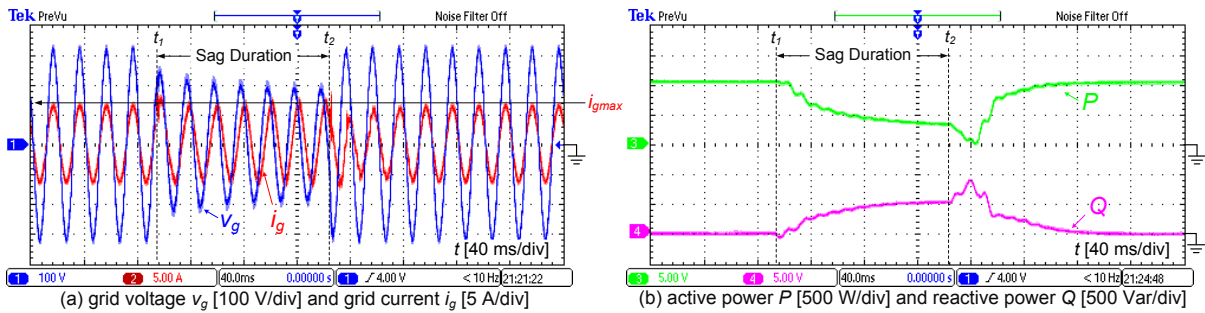


Fig. 9. Experimental results of a 1 kW single-phase grid-connected system in low voltage ride through operation modes (0.43 p.u. voltage sag): grid voltage  $v_g$  [100 V/div]; grid current  $i_g$  [5 A/div]; active power  $P$  [500 W/div]; reactive power  $Q$  [500 Var/div]; time [40 ms/div].

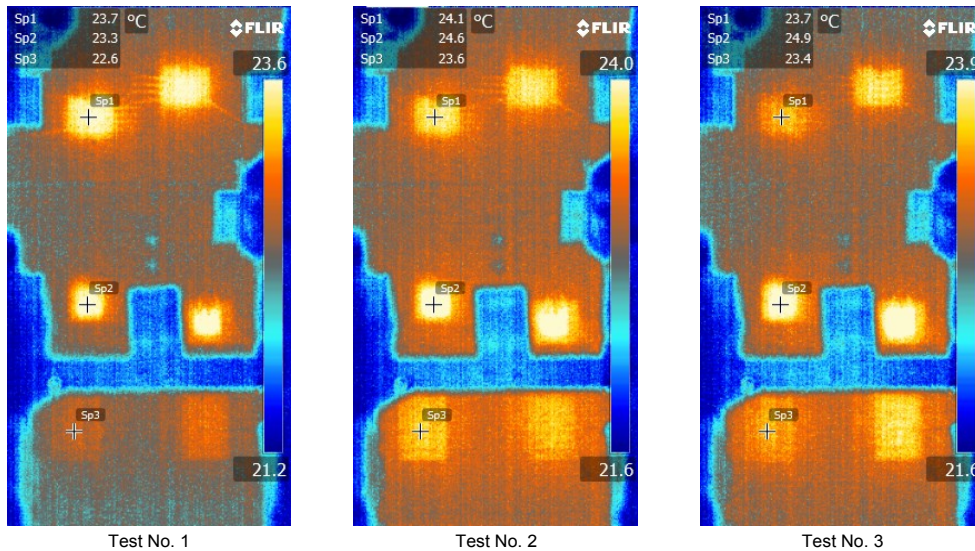


Fig. 10. Experimental results (thermal performance) of a single-phase 3-level NPC PV inverter under different power factors: Sp1 – IGBT, Sp2 – Clamped Diode and Sp3 – MOSFET.

experimental test shows that, by injecting reactive power, a constant amplitude of the grid current is achieved, leading to a reduced junction temperature as discussed above. It also demonstrates the flexibility of a single-phase system to provide multi-functionalities in the future. The single-phase  $PQ$  power control method in the test is effective in terms of fast dynamic response and reduced thermal stress. Furthermore, the dynamic behaviors of the active power and reactive power shown in Fig. 9(b) are similar to those in Fig. 8 during the voltage recovery period (i.e. voltage sag is cleared), which shows the effectiveness of the proposed junction temperature control method.

Since the lack of open IGBT modules and thus the corresponding thermal testing setup for the 3 kW single-phase PV inverter, of which many efforts will be devoted to in the future, the illustration of the junction temperature controllability is experimentally demonstrated on a 3-level NPC high power PV inverter operating at low power conditions. A commercial 3-level NPC PV inverter with the rated current of 30 A and the rated voltage of 1200 V is selected as the candidate for thermal tests, and each leg of the NPC inverter consists of two IGBTs, two clamped diodes and two MOSFETs. The switching frequency is 20 kHz and the experimental results are shown in Fig. 10 and Table IV. As it is observed in the test results, the junction temperature of the clamped diode (i.e. hotspot Sp2) experienced a linear change with the power factor, which is in coincidence with discussions presented in [28]. While the junction temperature of the IGBT is kept the same, but the power

factors are different (Test No. 1 and No. 3). This verifies the possibility to achieve a constant (or reduced) junction temperature of the power devices by appropriately allocating the active power and reactive power, which is the essential idea of this paper.

Table IV.  
TEST RESULTS OF A SINGLE-PHASE 3-LEVEL NPC PV INVERTER UNDER DIFFERENT POWER FACTORS.

Test No.	Power Factor	$P$ (W)	$Q$ (Var)	$S$ (VA)	Hotspot Temperature (°C)		
					Sp1	Sp2	Sp3
1	0.4538	257.4	505.5	567.3	23.7	23.3	22.6
2	0.8955	507.5	252.3	566.8	24.1	24.6	23.6
3	0.9996	564.7	16.8	565	23.7	24.9	23.4

#### IV. CONCLUSIONS

An approach to achieve a reduced or constant junction temperature of the switching devices in a single-phase PV inverter has been proposed in this paper. The controlled constant junction temperature and reduced temperature swings allow a further improved reliability of the PV inverter and an improved robustness of the PV system in response to abnormal grid conditions (e.g. low-voltage ride-through). By appropriately injecting reactive power to the grid during ride-through operation, the single-phase PV inverter would not be at the risk

of over-current protection and therefore with a better grid support capability. Simulation results on a 3 kW PV inverter with different levels of reactive power injection and experimental results from a 1 kW prototype verified the effectiveness of the presented control scheme. The proposed control method has been also demonstrate on a 3-level NPC PV inverter, and the results confirmed the controllability of the junction temperature through the injected power regulation. Considering that the voltage fault is a short period, the proposed method also offers the possibility to maintain a constant junction temperature of switching devices under varying solar irradiance levels if a wide range of reactive power injection is allowed by future grid codes.

#### REFERENCES

- 1 REN 21: 'Renewables 2013: Global Status Report (GSR)', <http://www.ren21.net/>, Jun. 2013
- 2 K.O. Kovanen: 'Photovoltaics and power distribution', *Renewable Energy Focus*, 2013, 14, (3), pp. 20-21
- 3 Malashenko, E., Appert, S., al-Mukdad, W.: 'Advanced inverter technologies Report' (California Public Utilities Commission, Jan. 2013), pp. 1-13
- 4 Carnieletto, R., Brandão, D.I., Suryanarayanan, S., Farret, F.A., Simões, M.G.: 'Smart grid initiative – A multifunctional single-phase voltage-source inverter', *IEEE Ind. Appl. Mag.*, 17, (5), 2011, pp. 27-35
- 5 Xue, Y., Divya, K.C., Griepentrog, G., Liviu, M., Suresh, S., Manjrekar, M.: 'Towards next generation photovoltaic inverters'. Proc. ECCE 2011, Phoenix, Arizona, Sept. 2011, pp. 2467-2474
- 6 Papanikolaou, N.P.: 'Low-voltage ride-through concept in flyback inverter-based alternating current-photovoltaic modules', *IET Power Electron.*, 2013, 6, (7), pp. 1436-1448
- 7 Yang, Y., Blaabjerg, F., Wang, H.: 'Low voltage ride-through of single-phase transformerless photovoltaic inverters', *IEEE Trans. Ind. Appl.*, 2014, Early Access at: <http://dx.doi.org/10.1109/TIA.2013.2282966>
- 8 Comitato Elettrotecnico Italiano, CEI 0-21: 'Reference technical rules for connecting users to the active and passive LV distribution companies of electricity', Dec. 2011
- 9 Bae, Y., Vu, T.-K., Kim, R.-Y.: 'Implemental control strategy for grid stabilization of grid-connected PV system based on german grid code in symmetrical low-to-medium voltage network', *IEEE Trans. Energy Convers.*, 2013, 28, (3), pp. 619-631
- 10 El Moursi, M.S., Xiao, W., Kirtley, J.L.: 'Fault ride through capability for grid interfacing large scale PV power plants', *IET Gener. Transm. Distrib.*, 2013, 7, (9), pp. 1027-1036
- 11 Benz, C.H., Franke, W.-T., Fuchs, F.W.: 'Low voltage ride through capability of a 5 kW grid-tied solar inverter'. Proc. EPE-PEMC 2010, Ohrid, Republic of Macedonia, Sept. 2010, pp. T12-13-T12-20
- 12 Kjaer, S.B., Pedersen, J.K., Blaabjerg, F.: 'A review of single-phase grid-connected inverters for photovoltaic modules', *IEEE Trans. Ind. Appl.*, 2005, 41, (5), pp. 1292-1306
- 13 Meneses, D., Blaabjerg, F., García, O., Cobos, J.A.: 'Review and comparison of step-up transformerless topologies for photovoltaic AC-module application', *IEEE Trans. Power Electron.*, 2013, 28, (6), pp. 2649-2663
- 14 Miret, J., Camacho, A., Castilla, M., Garcia de Vicuna, J., Matas, J.: 'Control scheme with voltage support capability for distributed generation inverters under voltage sags', *IEEE Trans. Power Electron.*, 2013, 28, (11), pp. 5252-5262
- 15 Collins, E., Dvorack, M., Mahn, J., Mundt, M., Quintana, M.: 'Reliability and availability analysis of a fielded photovoltaic system'. Proc. PVSC 2009, Philadelphia, Pennsylvania, Jun. 2009, pp. 2316-2321
- 16 Wang, H., Liserre, M., Blaabjerg, F.: 'Toward reliable power electronics: challenges, design tools, and opportunities', *IEEE Ind. Electron. Mag.*, 2013, 7, (2), pp. 17-26
- 17 Huang, H., Mawby, P.A.: 'A lifetime estimation technique for voltage source inverters', *IEEE Trans. Power Electron.*, 2013, 28, (8), pp. 4113-4119
- 18 Sujod, M.Z., Erlich, I., Engelhardt, S.: 'Improving the reactive power capability of the DFIG-based wind turbine druing operation around the synchronous speed', *IEEE. Trans. Energy Convers.*, 2013, 28, (3), pp. 736-745
- 19 Muray, C.J., Davoudi, A., Chapman, P.L.: 'Reliability analysis for single-phase photovoltaic inverters with reactive power support'. Proc. PECE 2011, Champaign, Illinois, Feb. 2011, pp. 1-6
- 20 Petrone, G., Spagnuolo, G., Teodorescu, R., Veerachary, M., Vitelli, M.: 'Reliability issues in photovoltaic power processing systems', *IEEE Trans. Ind. Electron.*, 2008, 55, (7), pp. 2569-2580
- 21 Harb, S., Balog, R.S.: 'Reliability of candidate photovoltaic module-integrated-inverter (PV-MII) topologies—a usage model approach', *IEEE Trans. Power Electron.*, 2013, 28, (6), pp. 3019-3027
- 22 De Leon-Aldaco, S.E., Calleja, H., Chan, F., Jimenez-Grajales, H.R.: 'Effect of the mission profile on the reliability of a power converter aimed at photovoltaic applications—a case study', *IEEE Trans. Power Electron.*, 2013, 28, (6), pp. 2998-3007
- 23 Hitachi, Ltd.: 'High Voltage IGBT Module Application Manual', Dec. 2009, pp. 1-33
- 24 Dieckerhoff, S., Bernet, S., Krug, D.: 'Power loss-oriented evaluation of high voltage IGBTs and multilevel converters in transformerless traction applications', *IEEE Trans. Power Electron.*, 2005, 20, (6), pp. 1328-1336
- 25 Dupont, L., Avenas, Y., Jeannin, P.-O.: 'Comparison of junction temperature evaluations in a power IGBT module using an IR camera and three thermosensitive electrical parameters', *IEEE Trans. Ind. Appl.*, 2013, 49, (4), pp. 1599-1608
- 26 Ji, B., Pickert, V., Cao, W., Zahawi, B.: 'In Situ diagnostics and prognostics of wire bonding faults in IGBT modules for electric vehicle drives', *IEEE Trans. Power Electron.*, 2013, 28, (12), pp. 5568-5577
- 27 Ma, K., Blaabjerg, F.: 'Modulation methods for neutral-point-clamped wind power converter achieving loss and thermal redistribution under low-voltage ride-through', *IEEE Trans. Ind. Electron.*, 2014, 61, (2), pp. 835-845
- 28 Ma, K., Liserre, M., Blaabjerg, F.: 'Reactive power influence on the thermal cycling of multi-MW wind power inverter', *IEEE Trans. Ind. Appl.*, 2013, 49, (2), pp. 922-930
- 29 Murdock, D.A., Ramos Torres, J.E., Connors, J.J., Lorenz, R.D.: 'Active thermal control of power electronics modules', *IEEE Trans. Ind. Appl.*, 2006, 42, (2), pp. 552-558
- 30 Yang, Y., Wang, H., Blaabjerg, F., Ma, K.: 'Mission profile based multi-disciplinary analysis of power modules in single-phase transformerless photovoltaic inverters'. Proc. EPE'13 ECCE Europe 2013, Lille, France, Sept. 2013, pp. P.1-P.10
- 31 Wagenitz, D., Hambrecht, A., Dieckerhoff, S.: 'Lifetime evaluation of IGBT power modules applying a nonlinear saturation voltage observer'. Proc. CIPS 2012, Nuremberg, Germany, Mar. 2012, pp. 1-5
- 32 Lutz, J., Schlangenotto, H., Scheuermann, U., De Doncker, R.: 'Semiconductor Power Devices: Physics, Characteristics, Reliability' (Springer, 2011)
- 33 ABB: 'Application Note: Applying IGBTs', May 2012, pp. 1-40
- 34 ON Semiconductor: 'IGBT Applications (Handbook)', Jul. 2012
- 35 Plexim: 'The simulation platform for power electronic systems (User Manual Version 3.4)', <http://www.plexim.com/download/documentation>, Jun. 2013